Journal of Alloys and Compounds 376 (2004) 180–185

Journal of ALLOYS AND COMPOUNDS

www.elsevier.com/locate/jallcom

Hydrogen production and crystal structure of ball-milled MgH_2–Ca and MgH_2–CaH_2 mixtures

J.-P. Tessier[a], P. Palau[a,1], J. Huot[b,2], R. Schulz[b], Daniel Guay[a,*]

[a] *Lab. de Recherche Mat. Avances, INRS Énergie, Matériaux et Télécommunications, Université de Québec, 1650 Boul. Lionel-Boulet, C.P. 1020, Varennes, Que., Canada J3X 1S2*

[b] *Expertise Chimie et Matériaux, Institut de Recherche d'Hydro-Québec, 1800 Boul. Lionel-Boulet, Varennes, Que., Canada J3X 1S1*

Received 15 November 2003; received in revised form 8 December 2003; accepted 8 December 2003

Abstract

The structure and hydrolysis reaction of ball-milled MgH_2–Ca and MgH_2–CaH_2 mixtures was investigated in function of milling time and component proportion. The nanocomposites formed by milling show faster hydrolysis reaction as well as higher hydrogen yield compared to conventional polycrystalline materials. This improvement is due to the formation of calcium hydride upon milling and to the fine mixture that results from extensive milling. When the milling is performed on MgH_2–20.3 mol% CaH_2 mixtures, the reaction yield reaches 80% after 30 min of hydrolysis.

Keywords: Chemical hydrides; Nanocrystalline materials; Hydrolysis; Irreversible hydrides

1. Introduction

For widespread utilization of hand-portable proton exchange membrane fuel cell (PEMFC), a compact, safe and inexpensive source of hydrogen must be designed. Hydrolysis reactions could potentially serve this purpose. However, for most compounds, the reaction is either too violent (for example: $LiAlH_4$) or too slow to be convenient. Also, because of the practical non-reversibility of this means of generating hydrogen, the chosen materials should be of low cost.

Chemical hydrides such as sodium borohydride ($NaBH_4$) or lithium aluminum hydride ($LiAlH_4$) can be used as hydrogen generators [1]. However, one important drawback of this method is the need of using a catalyst to activate the reaction [2–4]. Recently, Matthews and coworkers [5,6] have investigated novel complex hydrides stabilized with organic ligands as a source of hydrogen for PEMFCs. Hydrogen production by steam hydrolysis of $NaBH_4$ was also investigated and found to meet the purity requirement for fuel cell applications [7]. However, the price and availability of these types of compounds may make their widespread use difficult. Therefore, there is a need for the development of an inexpensive chemical hydride which has high hydrogen yield, and fast but controllable hydrogen release. Furthermore, the residual products should be environmentally friendly.

In a previous paper it was shown that, compared to conventional materials, MgH_2–Ca nanocomposites have hydrolysis kinetics greatly enhanced as well as much higher yield of reaction [8]. In this paper, we present a systematic investigation of the structure and hydrolysis characteristics of ball-milled MgH_2–Ca and MgH_2–CaH_2 mixtures. Depending on the phases present in the synthesized nanocomposites, the chemical reactions of interest are:

$$Mg + 2H_2O \rightarrow Mg(OH)_2 + H_2 \quad (1)$$

$$MgH_2 + 2H_2O \rightarrow Mg(OH)_2 + 2H_2 \quad (2)$$

$$Ca + 2H_2O \rightarrow Ca(OH)_2 + H_2 \quad (3)$$

$$CaH_2 + 2H_2O \rightarrow Ca(OH)_2 + 2H_2 \quad (4)$$

---

[*] Corresponding author. Tel.: +1-450-929-8141; fax: +1-450-929-8102.

E-mail addresses: huot.jacques@ireq.ca (J. Huot), guay@inrs-emt.uquebec.ca (D. Guay).

[1] Present address: Pechiney Centre de Recherches de Voreppe, 725 rue A. Berges, BP 27, 38341 Voreppe Cedex, France.

[2] Co-corresponding author.

0925-8388/$ – see front matter © 2004 Elsevier B.V. All rights reserved.
doi:10.1016/j.jallcom.2003.12.013

2. Experimental details

The nanocomposites were synthesized by first mixing the raw materials inside an argon filled glove box. The mixtures were then milled in a Spex 8000 model shaker mill using a vial and balls made of stainless steel, with a ball to powder weight ratio of 8:1. Magnesium hydride from Th. Goldschmidt (95 wt.% MgH_2, 5 wt.% Mg), calcium (Alfa, 98.8%), and CaH_2 powder (Aldrich, 95%) were used. In an earlier work on ball-milled magnesium hydride, it was found that the milled powder contains a significant (8 wt.%) fraction of magnesium oxide [9]. Because this oxide does not participate in the hydrolysis reaction, it was subtracted in all calculations of the theoretical yields of the reaction.

The hydrolysis reactions were carried out in a 1 l glass reactor with four openings used for hydrogen exhaust, water addition, thermometer, and purge gas. Water addition was made using a 250 ml ampoule provided with a bypass duct to prevent gas flow during water addition. The exhaust gas was flown through a condenser followed by drierite in order to remove all water vapors. The dry hydrogen gas was then directed to a flow meter (ADM 2000, Agilent Technologies) where the flow was measured. In each experiment, a mass of about 250 mg of nanocomposite was loaded into the flask and allowed to react with 100 ml of deionized water. The water addition was performed at $t = 1$ min in order to establish a background reading of the flow meter. This background ($\approx 0.29\,\mathrm{ml\,min^{-1}}$) was subsequently subtracted from the raw data. For all measurements, a magnetic stirrer was used to continuously stir the mixture. In order to easily compare the different measurements, hydrogen releases is given as reacted fraction, F, defined as the ratio of the volume of released hydrogen over the theoretical volume of hydrogen that should be released assuming that all material is hydrolyzed. For each experiment, the mass of reactant is 250 ± 5 mg and water volume is 100 ml.

The pH was measured with a pH meter from VWR Scientific model 2000, using an Accumet 13-620-108 electrode. The specific surface area was measured with an Autosorb 1 gas sorption system from Corporation Quantachrome using the BET method with nitrogen gas.

X-ray powder diffraction was carried out on a Bruker AXS D8 diffractometer using Cu Kα radiation. Crystallite size of magnesium hydride was evaluated using TOPAZ 2 software to fit the (1 1 0) peak of magnesium hydride.

3. Results and discussion

3.1. Effect of Ca proportion

The effect of Ca proportion in 10 h ball-milled MgH_2–Ca nanocomposites is shown in Fig. 1. For comparison, ball-milled MgH_2 without Ca addition and polycrystalline MgH_2 are also shown. All curves showed a very fast initial reaction which lasts from 30 s to 1 min. The nature of this first step is given by examination of the pure MgH_2 curves. In this case, the reaction stops after about 1 min. Independent measurements of the solution pH show that it reaches 10.5 in the first few minutes of hydrolysis. From the potential–pH equilibrium diagram, the concentration of the soluble species (Mg^{2+}) of reaction (1) is only 10^{-4} molar at pH 10.5 [10]. Therefore, after only 1 min of hydrolysis, the pH of the solution is already high enough to reduce the solubility of Mg^{2+} to negligible value. This may explain the sudden stop of the initial burst of the reaction, as the formation of insoluble magnesium hydroxide at the surface of the grains will prevent the solution from reaching un-reacted MgH_2. There is almost twice as much hydrogen liberated from MgH_2 milled during 10 h compared to polycrystalline MgH_2. This most probably arises as a consequence of the former material having a higher effective surface area than the later one (9.7 and 1.2 $m^2\,g^{-1}$, respectively).

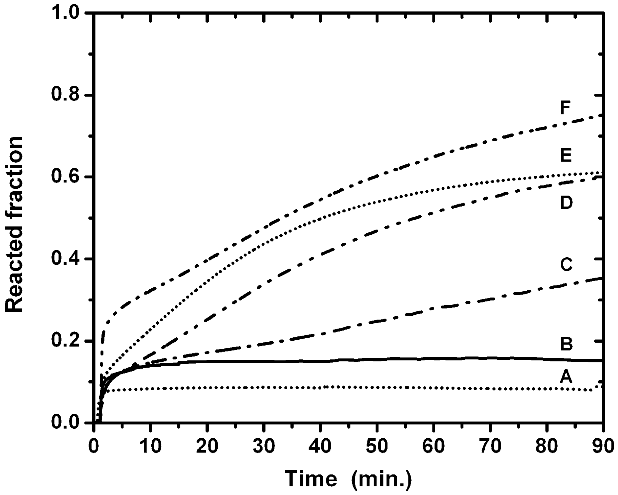

Fig. 1. Hydrogen released during hydrolysis of (A) polycrystalline MgH_2, (B) MgH_2 milled 10 h, MgH_2–X mol% Ca nanocomposite milled 10 h with (C) $X = 4.7$ mol%, (D) $X = 8.9$ mol%, (E) $X = 20.3$ mol%, and (F) pre-milled MgH_2–20.3 mol% Ca milled 10 h.

With calcium addition, the fast initial step is followed by a constant hydrogen flow regime and the reacted fraction increases with time. In this regime, the calcium addition allows a sustained reaction of magnesium hydride, thus giving a faster kinetics and higher yield. From Fig. 1, we could see that the second slope is proportional to the calcium content, with higher calcium proportion producing higher flow rates and higher yield. However, at the highest calcium contents (8.9 and 20.3 wt.%), a third regime appears where the flow rate seems to be inversely proportional to the calcium content and the reacted fraction seems to level off. Moreover, the inflexion point, where the hydrogen release curve switches from the second to the third regime, is appearing sooner for higher calcium proportion. For calcium content of 8.9 and 20.3 mol%, the inflexion points are estimated to be 50 and 35 min, respectively. The curve with 4.7 mol% Ca does not show the third regime.

Table 1
Specific surface area of MgH_2–Ca mixtures ball-milled 10 h

Composition	Specific surface area ($m^2\,g^{-1}$)
Un-milled MgH_2	1.2
MgH_2	9.7
MgH_2–4.7 mol% Ca	7.1
MgH_2–8.9 mol% Ca	5.8
MgH_2–20.3 mol% Ca	3.4

One consequence of ball-milling is the variation of specific surface area of the milled material. In Table 1, the specific surface area of ball-milled MgH_2–Ca composites with various calcium contents is reported. Magnesium hydride being a brittle material, milling without additive produced an almost 10-fold increase of the specific surface area. When calcium is added, it acts as a binder thus reducing the specific surface area in direct proportion of the calcium content. From Table 1, it is clear that the specific surface area is not responsible for the enhanced reaction kinetic and reaction yield of MgH_2–Ca mixtures compared to ball-milled MgH_2. However, the leveling off of the reacted fraction at high Ca content may be related to the reduction of the surface area.

3.2. Phase composition

The phase composition of ball-milled MgH_2–Ca mixtures is revealed by the X-ray powder diffraction patterns shown in Fig. 2. The sample without calcium shows the characteristic diffraction peaks of β-MgH_2 as well as those indicating the presence of metastable γ-MgH_2 formed by energetic ball-milling [11]. The diffraction peaks are broad, pointing to the fact that these compounds are in a nanocrystalline form. More details about this material are given elsewhere [9]. For small proportion of calcium (4.7 mol%), the diffraction pattern shows a reduction of the γ-MgH_2 metastable phase and the appearance of a shoulder near 37 degrees. This shoulder corresponds to the most intense peak of the magnesium pattern. For higher calcium content (8.9 mol%), the γ-MgH_2 phase is almost totally extinct and the magnesium peaks are more apparent. At the highest calcium content prepared in this investigation (20.3 mol%), the γ-MgH_2 phase is absent, the magnesium peaks are better defined and peaks corresponding to CaH_2 are clearly present, with the main peaks located close to 30.5°. Therefore, upon milling of a MgH_2–Ca mixture, hydrogen atoms are transferred from MgH_2 to Ca, leading to the formation of CaH_2 and Mg. The nanocomposite thus formed should be written MgH_2–CaH_2 with inclusion of Mg phase. This reaction was expected as the enthalpy of formation of CaH_2 is $-188.7\,kJ\,mol^{-1}$ [12] compared to $-71.2\,kJ\,mol^{-1}$ for MgH_2 [13]. The fact that γ-MgH_2 is absent from the nanocomposite with the higher Ca content suggests that this phase reacts preferentially with Ca to form CaH_2 and Mg. This is consistent with the fact that γ-MgH_2 is less stable than β-MgH_2 [14].

To support this assertion, an experiment was performed where MgH_2 was first ball-milled for 5 h in order to synthesize a large fraction of the γ-MgH_2 metastable phase. Calcium was then added in a proportion of 20.3 mol% and the mixture was further milled for 10 h. The X-ray powder diffraction pattern of that compound is shown in Fig. 2. There is a higher proportion of CaH_2 and Mg in

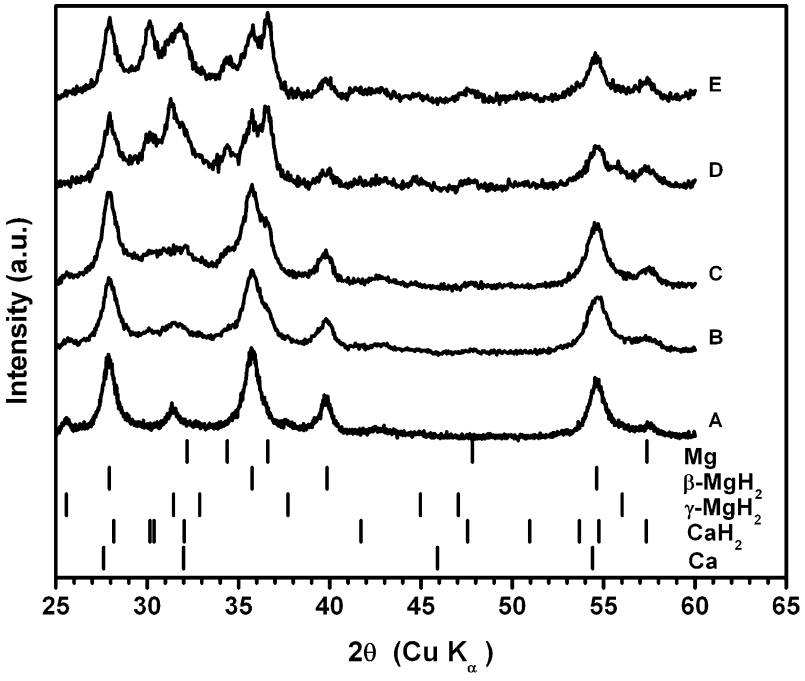

Fig. 2. X-ray powder diffraction patterns of MgH_2–X mol% Ca nanocomposite milled 10 h with (A) $X = 0.0$ mol%, (B) $X = 4.7$ mol%, (C) $X = 8.9$ mol%, (D) $X = 20.3$ mol%, and (E) pre-milled MgH_2–20.3 mol% Ca milled 10 h.

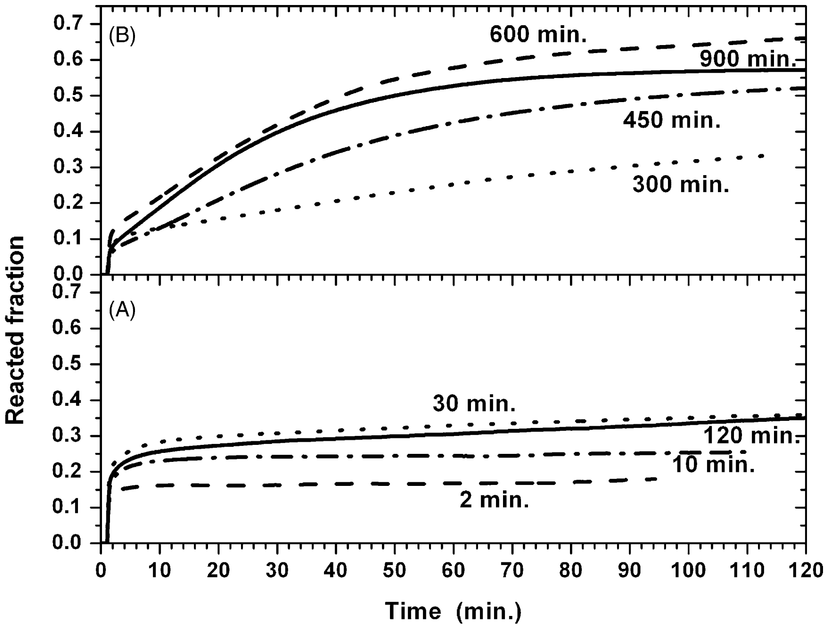

Fig. 3. Hydrogen released during hydrolysis of MgH_2–8.9 mol% Ca nanocomposite ball-milled for various durations.

the pre-milled sample, as indicated by the higher intensity of the diffraction peaks located at ∼30.5° and ∼37.0°, respectively. The hydrolysis curve of this material is shown in Fig. 1. It can be seen that pre-milled nanocomposite has a much bigger initial burst of hydrogen but afterward, for hydrolysis time between 1 and 40 min, the reaction is slower than in MgH_2–20.3 mol% Ca milled 10 h. For longer hydrolysis times, the reaction is faster for pre-milled materials. The higher initial burst could be explained by the higher proportion of CaH_2 in the pre-milled sample as evidenced in the X-ray powder diffraction pattern.

3.3. *Effect of milling time*

A systematic study of hydrogen release as a function of milling time was performed for the ball-milled mixture MgH_2–8.9 mol% Ca. The results are shown in Fig. 3. As revealed by Fig. 3A, for milling time shorter than 120 min, the reaction stops after the initial burst. The milling time has some effect on the magnitude of this initial burst, the reacted fraction increases with milling time until a maximum is reached for 30 min of milling. Further milling up to 120 min only slightly reduced the initial hydrogen release.

Longer milling times are shown in Fig. 3B. For 300 min milling, the initial burst is followed by a second regime of constant flow rate. When milling is performed for 450 min or more, this second regime gives way to a third regime of smaller flow rate. The transition from the second to the third regime is around 50 min for the 450 min milled sample and about 40 min for both 600 and 900 min milled samples. Therefore, the transition point seems to be function of calcium content (see Fig. 1) and milling time (see Fig. 3), with an optimum value for each of them.

The evolution of the solution pH during the hydrolysis reaction of MgH_2–8.9 mol% Ca milled 450 min is shown on Table 2. The pH increases very quickly and stabilizes to values superior to 11 after a few min of hydrolysis. In the same conditions, the end values of pH for hydrolysis of pure MgH_2 and pure Ca are, respectively, 10.5 and 12.3.

The X-ray powder diffraction patterns of ball-milled MgH_2–8.9 mol% Ca are shown in Fig. 4. After 60 min of milling, the structure is nanocrystalline as indicated by the broad peaks in the diffraction pattern. Peaks could be indexed to β-MgH_2 and γ-MgH_2 magnesium hydrides. Magnesium and calcium hydride peaks are also relatively strong, indicating that the decomposition of magnesium hydride occurs at the beginning of the milling process. The relative intensities of the diffraction peaks do not vary with milling time, suggesting that the sample's composition does not evolve with time after the initial 60 min of milling. On these premises, a variation of composition with milling time could hardly explain the difference of reaction yield and reaction kinetics observed between samples milled for different periods of time (see Fig. 3).

Table 2
Solution pH as a function of hydrolysis time of MgH_2–8.9 mol% Ca milled 450 min

Hydrolysis time (min)	pH
0	6.8
1	10.8
8	11.2
19	11.5
30	11.3
45	11.4
78	11.1

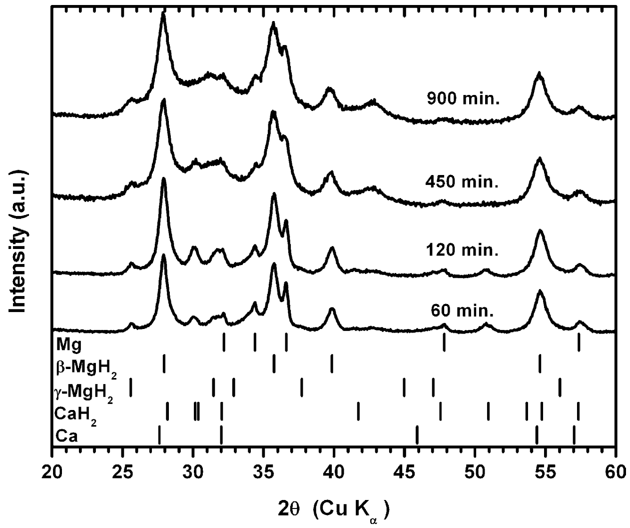

Fig. 4. X-ray powder diffraction patterns of MgH_2–8.9 mol% Ca ball-milled for different milling times.

The evolution of crystallite size of the β-MgH_2 phase as a function of milling time is shown in Table 3. Starting from the polycrystalline material, an important reduction of crystallite size is achieved after the first hour of milling. The final crystallite size is reached after 7.5 h of milling. It is interesting to note that higher reaction yield and faster reaction kinetics are reached as crystallite sizes are reduced during extensive milling.

The idea that compounds with similar composition but different structure (nanostructure) can exhibit largely varying reaction yield and reaction kinetics is best illustrated by the hydrolysis of less complex systems. A mixture of $MgH_2 + 20.3$ mol% CaH_2 was milled for 5 min and 10 h. Since Ca is present in the initial mixture in the form of a hydride, no reaction with MgH_2 is expected. This is confirmed by the X-ray powder diffraction pattern of the later compound (not shown) that displays only the characteristic peaks of MgH_2 and CaH_2. Milling for duration as short as 5 min does not change the structure of the material and serves only to mix the two raw components, while milling for 10 h reduces the crystallite size of both hydrides and favors the development of an intimate mixture down to the nanometer level.

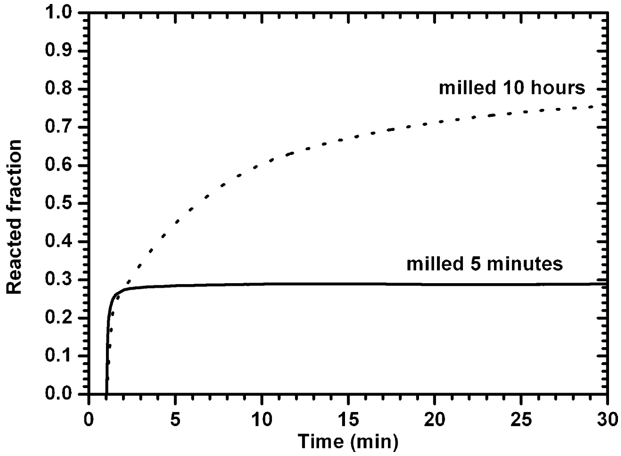

Fig. 5. Hydrogen released during hydrolysis of MgH_2–20.3 mol% CaH_2 nanocomposite ball-milled for 5 min and 10 h.

Hydrolysis curves of $MgH_2+20.3$ mol% CaH_2 are shown in Fig. 5. The sample milled for 5 min shows a hydrolysis reaction that stops after the initial reaction burst. A reaction yield of ∼0.3 is consistent with CaH_2 being fully hydrolyzed ($F = 0.2$), while the F value of polycrystalline MgH_2 is close to 0.1 (see Fig. 1). On the other hand, the hydrolysis reaction of a composite with the same initial composition but milled for a longer period of time proceeds at a much faster rate after the initial burst. In that later case, the reaction yield reaches ∼0.8 after 30 min of reaction. Since this compound contains only 20.3 mol% of CaH_2, such a high reaction yield cannot be explained by assuming that only CaH_2 is hydrolyzed (in that case, the reaction yield would have been 0.2). Indeed, close to 75% of MgH_2 present in the $MgH_2 + 20.3$ mol% CaH_2 nanocomposite milled 10 h must have reacted to get a reaction yield close to 0.8. This is quite surprising considering that the solution pH reaches values larger than 11.0 after only one or 2 min of reaction. In conventional materials, reduced solubility of Mg^{2+} and formation of a passivation layer effectively stop the hydrolysis reaction after a few minutes of reaction. However, in nanocrystalline materials with the same composition, the reaction proceeds almost to completion even at this low solubility level of Mg^{2+}.

Table 3
Crystallite size of magnesium hydride as a function of milling time of MgH_2–8.9 mol% Ca mixture

Milling time (h)	Crystallite size (nm)
1	42
2	35
5	24
7.5	17
15	16

It seems that there are two requirements for the hydrolysis reaction of MgH_2-based compounds to proceed through near completion. Firstly, MgH_2 should be mixed with a Ca compound, either in the form of a metal or a hydride. In the first case, prolonged milling of MgH_2 with Ca leads to the in situ formation of CaH_2. It is believed that the synergetic effect occurring in MgH_2+CaH_2 milled for 10 h is the same as that responsible for the higher reaction yield and faster reaction kinetics observed in MgH_2 + Ca nanocomposite. Secondly, as evidenced by the data of Fig. 5, the mixing between MgH_2 and CaH_2 should be thorough and should occur at the nanometer level.

The exact nature of the synergistic effect between MgH_2 and CaH_2 is not clear. Under our experimental conditions, calcium hydride is more readily hydrolyzed than MgH_2 and this reaction may be beneficial to open up the structure of

MgH_2 and favors the interaction between freshly exposed MgH_2 surface and the electrolyte. Also, the fact that the initial burst of hydrogen in the most active compound is followed by a period of time where the hydrogen flow is significant points to the fact that the passivation layer that is formed at the surface of MgH_2 grains must be different from that formed on pure MgH_2. The presence of CaH_2 and Ca^{2+} ions in the vicinity of MgH_2 must influence the composition, the structure and the permeability of the passivation layer, thereby allowing the hydrolysis reaction on MgH_2 to proceed to a greater extent than observed in the case of pure MgH_2. The nanostructure that develops in the composite upon extensive milling is essential in obtaining high reaction yields and fast kinetics of the hydrolysis reaction.

4. Conclusion

A systematic investigation of the structure and hydrolysis characteristics of ball-milled MgH_2–Ca and MgH_2–CaH_2 mixtures was carried out. It was found that when a mixture of magnesium hydride and calcium is milled, calcium hydride is formed by the transfer of hydrogen from magnesium hydride. The resulting nanocomposite Mg–MgH_2–CaH_2 has faster hydrolysis kinetics and higher yield compared to ball-milled pure magnesium hydride. Thus, calcium addition allows a faster and more complete hydrolysis reaction of magnesium hydride. Even if calcium hydride is formed during milling, faster hydrolysis reaction and higher yield are achieved when calcium hydride is used directly as starting component instead of calcium. In the case of $MgH_2 + 20.3$ mol% CaH_2 milled during 10 h, the reaction yield is close to 0.8 after 30 min of hydrolysis. In that later case, 75% of the MgH_2 initially present in the composite is decomposed after 30 min of hydrolysis.

References

[1] H.I. Schlesinger, H.C. Brown, A.E. Finholt, J.C. Gilbreath, H.R. Hoekstra, E.K. Hyde, J. Am. Chem. Soc. 75 (1953) 215–219.
[2] S.C. Amendola, M. Binder, S.L. Sharp-Goldman, M.T. Kelly, US Patent 6534033 B1, 2003.
[3] S.C. Amendola, S.L. Sharp-Goldman, M.S. Janjua, N.C. Spencer, M.T. Kelly, P.J. Petillo, M. Binder, Int. J. Hydrogen Energy 25 (2000) 969–975.
[4] S. Suda, Y.-M. Sun, B.-H. Liu, Y. Zhou, S. Morimitsu, K. Arai, N. Tsukamoto, M. Uchida, Y. Candra, Z.-P. Li, Appl. Phys. A 72 (2001) 209.
[5] J.E. Stearns, M.A. Matthews, D.L. Reger, J.E. Collins, Int. J. Hydrogen Energy 23 (1998) 469–474.
[6] R. Aiello, M.A. Matthews, D.L. Reger, J.E. Collins, Int. J. Hydrogen Energy 23 (1998) 1103–1108.
[7] R. Aiello, J.H. Sharp, M.A. Matthews, Int. J. Hydrogen Energy 24 (1999) 1123–1130.
[8] J. Huot, G. Liang, R. Schulz, J. Alloys Compd. 353 (2003) L12–L15.
[9] J. Huot, G. Liang, S. Boily, A.V. Neste, R. Schulz, J. Alloys Compd. 293–295 (1999) 495–500.
[10] M. Pourbaix, Atlas of Electrochemical Equilibria in Aqueous Solution, NACE International, Cebelcor, 1974.
[11] J. Huot, G. Liang, R. Schulz, Appl. Phys. A 72 (2001) 187–195.
[12] D.R. Lide (Editor-in-Chief), Handbook of Chemistry and Physics, 77th ed., 1996–1997.
[13] J.J. Reilly, R.H. Wiswall, K.C. Hoffman, C.H. Waide, BNL 18867 (1974).
[14] A.R. Yavari, J.F.R. de Castro, G. Vaughan, G. Heunen, J. Alloys Compd. 353 (2003) 246–251.